Effect of Pretreatment Variables on the Reaction of Nitric Oxide (NO) with Au−TiO_2: DRIFTS Studies

Mahlaba A. Debeila,[†] Neil J. Coville,[†] Mike S. Scurrell,*[,†] Giovanni R. Hearne,[‡] and Mike J. Witcomb[§]

Molecular Sciences Institute, School of Chemistry, Private Bag X3, University of the Witwatersrand, Johannesburg 2050, South Africa, Mössbauer Laboratory, School of Physics, Private Bag X3, University of the Witwatersrand, Johannesburg 2050, South Africa, and Electron Microscope Unit, Private Bag X3, University of the Witwatersrand, Johannesburg 2050, South Africa

Received: March 12, 2004; In Final Form: August 30, 2004

The effect of the pretreatment on the interaction between NO and Au−TiO_2 was examined using DRIFTS as a monitoring tool. For calcined and reduced Au−TiO_2, adsorption of NO on the TiO_2 support is not promoted under the conditions employed. $Au(NO)_2$ is the predominant species on oxidized and reduced Au−TiO_2 with initial bands at 1818 and 1740 cm^{-1}. Analysis showed that these species are sensitive to the surface coverage, temperature, and the state of the underlying surface, shifting from 1820 cm^{-1} for reduced Au−TiO_2 to 1850 cm^{-1} for oxidized Au−TiO_2 and from 1740 to 1734 cm^{-1} with increasing surface temperature. It is proposed that different dinitrosyl components are formed on the surface and are bonded to Au sites in different chemical environments. Small dissociative contributions (N_2O formation) were detected at higher NO pressures and temperatures. Adsorption of NO on oxidized Au−TiO_2 is dominated by bridging NO adsorbates (bands at 1665 and 1641 cm^{-1}) at low NO exposures, but linearly bound NO (bands at 1873, 1860, 1838, and 1808 cm^{-1}) were detected with increasing NO coverage. Products of dissociation and associated mainly with the TiO_2 support dominate the spectra for oxidized Au−TiO_2.

Introduction

Small gold particles supported on different oxide supports, for example, TiO_2, ZrO_2, and Al_2O_3, are active for low-temperature CO oxidation.[1,2] However, the activity of supported gold catalysts is affected by preparation conditions and the size of the gold particles.[3−5] Though impregnated gold catalysts could become active following sequential high-temperature reduction (773 K), calcination (673 K), and low-temperature reduction (473 K),[6−7] the preferred method for preparing gold catalysts seems to be deposition-precipitation.[8−10]

Pretreatment conditions for Au−TiO_2 play an important role in generating a high activity in this system.[5−7,12] For example, a catalyst initially pretreated in oxygen showed no activity even after subsequent hydrogen reduction.[12] However, a catalyst which has been reduced at 773 K retained activity after reoxidation at 773 K.[12]

Because of increasing social demands, more efforts have been devoted to clean polluted air for nitrogen oxides species from combustion processes such as automobile systems. Therefore, the study of the nitrogen oxides is important and research is extensively being carried out on the related subject of catalysis, including spectroscopic studies on nitrogen oxides adsorption on solid catalysts. Because of its high activity in the CO oxidation reaction, gold catalysts have also been studied for NO reduction and decomposition.[11]

Previous studies of NO adsorption on Au^I supported on zeolites unfortunately involved the immediate decomposition of NO already taking place at room temperature.[16−18] As a result of this, it was therefore not possible to study the nature of Au−NO bonding. In the supported gold catalysts, an additional complicating factor arises because the support materials may also be involved in the adsorption and decomposition of NO. Several different mechanisms for NO decomposition on other metal catalysts have been proposed.[13−15]

In this article, we have investigated the effect of the pretreatment on the adsorptive properties of Au−TiO_2. Using NO as a probe molecule, the surface species produced upon adsorption of NO on oxidized and oxidized/reduced Au−TiO_2 are identified.

It is shown that calcination followed by reduction of Au−TiO_2 promotes adsorption of NO exclusively onto Au containing sites. This predominant molecularly adsorbed NO (with virtually no other higher nitrogen oxo or N_yO_x species) offers an opportunity to study the nature of NO bonding and dissociation of NO in a controlled way. However, on oxidized Au−TiO_2, adsorption is nonselective, that is, adsorption occurs on both the Au and TiO_2 support and results in the formation of higher NO_x species as a result of the dissociation of NO and combination of NO with dissociated products. The importance of these surface complexes is discussed.

Experimental Section

DRIFTS spectra were recorded on a Nicolet Impact 420 IR spectrometer, equipped with a DTGS detector at a spectral resolution of 4 cm^{-1} as described elsewhere.[19] The fine powdered samples were loaded into a sample cell (Harrick Scientific) equipped with a ZnS window which allowed treatment of samples under various controlled atmospheres. Gases were supplied by Afrox Ltd.

* Corresponding author. E-mail: scurrell@Aurum.chem.wits.ac.za.
[†] Molecular Sciences Institute.
[‡] Mössbauer Laboratory.
[§] Electron Microscope Unit.

10.1021/jp048899k CCC: $27.50
Published on Web 10/29/2004

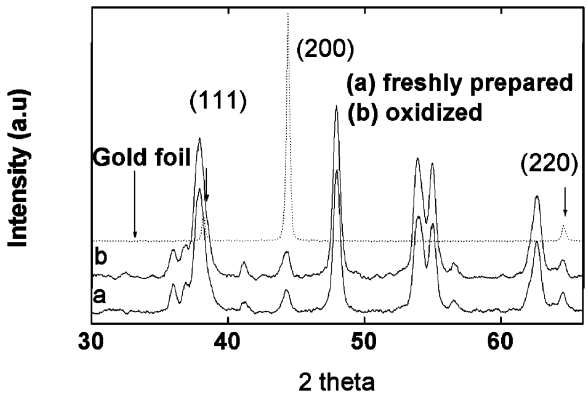

Figure 1. XRD of $Au-TiO_2$ for freshly prepared and calcined catalysts.

The catalyst was prepared by a standard precipitation procedure using $HAuCl_4$ and Degussa TiO_2 P-25 previously described.[19] A solution of deionized $HAuCl_4$ was adjusted to the required pH (pH 3.5−4) with vigorous stirring using 2 M solution of NH_4OH at room temperature. Once the required pH was obtained, the TiO_2 support was suspended in solution and the resulting mixture was stirred further for 30 min and then aged for 24 h. The water was removed by centrifuge and the solid catalyst was dried in an oven at 150 °C for 16 h. The catalyst was calcined (oxidized) at 400 °C in 5% O_2/He mixture at a flow rate of 30 mL/min for 2 h. DRIFTS spectra were recorded after the following pretreatments:

(i) The calcined catalyst was loaded into the DRIFTS cell and flushed with He (flow rate of 30 mL/min) and the temperature of the system was raised at a rate of 10°/min to 300 °C and held at this temperature for 2 h and then reduced to room temperature. Then NO was introduced. (ii) A new sample (calcined catalyst) was loaded into the IR cell and reduced with 50% H_2/Ar gas (a flow rate = 30 mL/min) at 300 °C for 2 h. After reduction, He was introduced at the reduction temperature and the catalyst was cooled to room temperature and NO was introduced. After each pretreatment, a background spectrum of the pretreated sample was measured at room temperature before commencement of NO adsorption measurements. About 500 scans were accumulated per run. The pressures quoted in this study are gauge pressures (not absolute pressures) unless otherwise indicated.

X-ray Powder Diffraction. The catalysts were crushed to a fine powder (∼<45 μM). A Phillips PW 1710 diffractometer, equipped with monochromator and Cu cathode ray tube, was used. A generator was operated at a voltage of 40 kV and a current of 20 mA. Samples were run in a continuous scan mode in the range 5−70 (in scales of 2θ), in step size of ∼0.020 (in scales of 2θ) with time per step of ∼1.0 s.

Transmission Electron Microscope (TEM). Transmission electron microscope measurement was carried out on Philips CM 200 operated at 197 keV.

Results

(a) Catalyst Characterization. The catalyst studied here was characterized by powder XRD diffraction and the patterns are depicted in Figure 1. The patterns show reflections at 32.2, 44.4, and 64.6° 2θ values characteristic of metallic gold. Comparison of the pattern with that of gold foil run under similar conditions shows that there are little or no line broadening in the profile for the $Au-TiO_2$ samples which would be characteristic of relatively small gold particles. This shows that the particles on this catalyst are large. This is confirmed by TEM (Figure 2). It can be seen that the majority of the particles are larger than 100 nm. In some cases, clusters were seen indicating the tendency of the particles to agglomerate.

(b) DRIFTS Measurements. *(i) Calcined Au/TiO₂.* To suppress as much as possible the sequential reactions of adsorbed NO, NO was introduced in small amounts to the oxidized $Au-TiO_2$ at ∼0.3 bar and the spectra measured following each addition (Figure 3a−e). Before increasing the NO pressure, the steady-state flow of NO was maintained (curve f). The recorded spectra for this catalyst are depicted in Figure 3 as a function of time (curves a−f) and increased gas pressure (curves f−h). Exposure of the catalyst to NO led to the development of numerous IR bands: 1656 (broad), 1574, 1529 (weak), 1474, 1419, 1369, 1337 (shoulder), and 1261 (broad) cm^{-1} (Figure 3a). The subsequent additions of NO led to changes in the spectra (Figure 3a−f). The broad band observed at 1656 cm^{-1} was replaced by two poorly resolved bands with distinguished maxima at 1665 and 1641 cm^{-1} (curves a−g). The band at 1641 cm^{-1} grew faster than that at 1665 cm^{-1}, which remained as a shoulder on the higher wavenumber side of this band. The weak band observed at 1574 cm^{-1} broadened and slightly grew (curves b−c) and seemed to decrease and shifted slightly to 1592 cm^{-1} (curves e−g). However, on increasing the pressure to 2 bar, a sudden appearance of the band at 1577 cm^{-1} was observed (curve h). The most intense band in the spectra is seen at 1483 cm^{-1} (curve h), shifted from an initial weak band at 1474 cm^{-1} (curves d−g). In the lower wavenumber region, bands developed and grew at 1441 (shoulder), 1380, 1328, and 1285 cm^{-1} (Figure 3h). In the nitrosyl stretching region (1900−1700 cm^{-1}), there is no feature corresponding to Au−NO complexes detected above the limit imposed by noise (Figure 3a−b). However, careful analysis of the spectra in this region shows that very low intensity band at ∼1850 cm^{-1} was detected on introduction of the sample to NO (Figure 3a−b). This band increased in intensity in subsequent additions of NO and slightly shifted to 1860 cm^{-1} (curve c). Further additions resulted in the development of low intensity shoulders on both sides of this band at ∼1910 and 1830 cm^{-1} (curve d). Further additions and increased pressure of NO resulted in the band at 1910 cm^{-1}, which grew to almost the same intensity as the band at 1860 cm^{-1} and slightly shifted to 1903 cm^{-1} (curve h). The bands in this region seem more complex and are shown in expanded scale in the insert in Figure 3. There it shows another low intensity shoulder at 1808−1810 cm^{-1}. Very low intensity bands also developed at 2235 and 2205 cm^{-1} with increased pressure of NO (curve h).

Various surface species adsorbed mainly on TiO_2 were detected and the assignments of these species have been discussed,[19−21] (see Table 1). The band at 1577 cm^{-1} is in a similar position to one of the bands detected over Au^I/NaY and assigned to adsorbed N_2O_3.[16−17] This complex has another component in the nitrosyl stretching region, 1907−1860 cm^{-1}, because of ν(N═O) and might be contained within the complex band in the region 1903−1860 cm^{-1} (Figure 3), and the ν_{sym}·(NO_2) is found in the region 1301 cm^{-1} and its observation might be obscured by other bands in this region with maxima at 1331 and 1286 cm^{-1}. Bands with vibrational frequencies in the region 1640−1670 cm^{-1} have not previously been detected on TiO_2 and therefore must be associated with Au containing sites. Bands in this region have previously been reported on various metal catalysts and are assigned to the vibrational frequency, ν(N−O) of NO adsorbed to the surface in different coordination states, for example, bent molecule[22−25] and bridged NO species.[26−27] Figure 3 shows that the bands (at 1665 and 1641 cm^{-1}) associated with these species are dominant in the

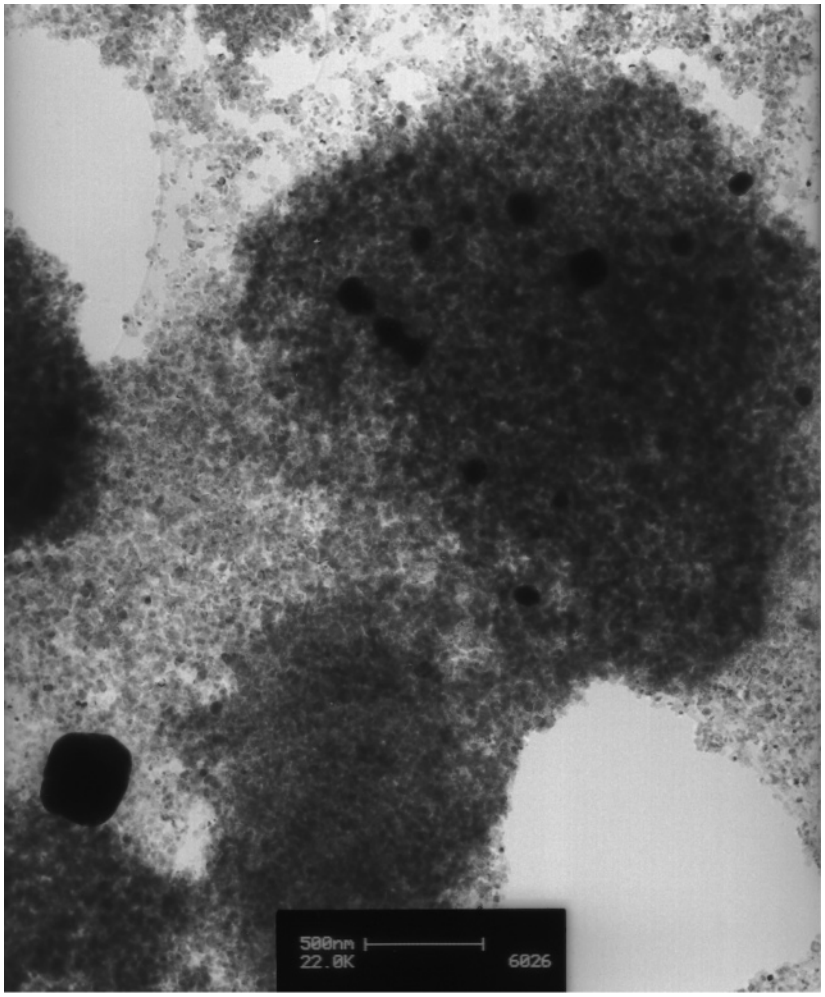

Figure 2. TEM image of Au particles on TiO_2 calcined at 400 °C.

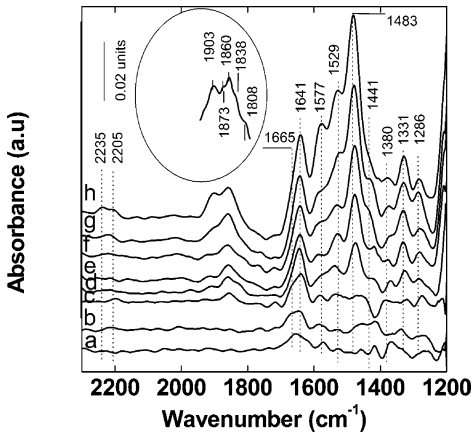

Figure 3. IR spectra of NO adsorbed on calcined $Au-TiO_2$. Gas (0.3% NO in He) was introduced at (a) room temperature, 0.3 bar, 15 min; (b) room temperature, 0.3 bar, 30 min; (c) room temperature, 0.3 bar, 45 min; (d) room temperature, 0.3 bar, 60 min (e) room temperature, 0.3 bar, 75 min; (f) room temperature, 0.3 bar, 105 min (flow mode); (g) room temperature, 1 bar, 120 min (flow mode); and (h) room temperature, 2 bar, 125 min (flow mode).

TABLE 1: Assignments of Various IR Bands to Different Surface Complexes

IR bands	possible assignments
1577	asym-N_2O_3 possibly adsorbed on Au sites
1592(sh)[a]	asym-N_2O_3 associated with TiO_2
1529	bridging nitrito surface species (NO_2^-)
1483	unidentate nitrito ($M-O-N=O^-$)
1441(sh), (1328)	nitro ($M-NO_2$) surface complexes
1380(w)	bridging nitrite or chelating nitrite surface complexes
1285	chelating nitrito surface complexes
1641, 1665	bridging NO adsorbates, $(Au)_x(NO)$
1808	linearly bound NO on metallic Au ($Au-NO^-$)
1838	linearly bound NO on metallic Au interacting with TiO_2 support ($O^{\delta-}-Au^{\delta+}-NO$)
1860	($O_2^{\delta-}-Au^{\delta2+}-NO$)
1873	weakly adsorbed NO on metallic gold ($Au^{\delta2+}$---NO)
1903	$TiO_2(NO)$
1810, 1740	$Au(NO)_2$
1850, 1734	($O_2^{\delta-}-Au^{\delta2+}(NO)_2$ NO bound to positively polarized gold sites
1620	δ(HOH)

[a] sh: shoulder, w: weak.

initial spectra (curves a−c), suggesting that the sites to which these NO molecules are bonded are populated first and represent the most stable NO adsorption sites on this catalyst at room temperature. It has been reported that at low coverage, NO is adsorbed in bridging sites and as the coverage increases the atop bound state is preferred.[28] In addition, since bridge-bonded NO adsorbates are multiply coordinated and more strongly adsorbed and the (bridging) sites are expected to be populated first,[29] the bands at 1665 and 1641 cm^{-1} are more likely to represent bridging NO entities. However, we are unable to determine whether these are twofold or threefold bridging sites or whether they bridge Au sites or Au and TiO_2 sites. However,

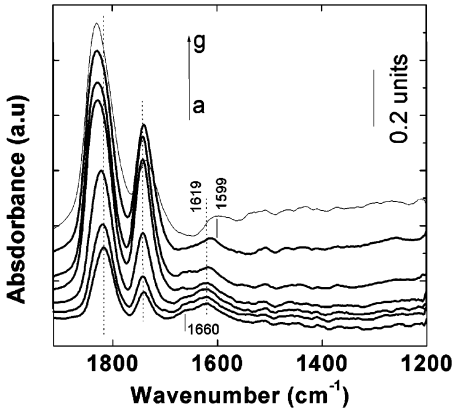

Figure 4. IR spectra of NO adsorbed on calcined and reduced Au−TiO_2. Gas (0.3% NO in He) was introduced at (a) room temperature, 1 bar, 15 min; (b) room temperature, 1 bar, 30 min; (c) room temperature, 1 bar, 45 min; (d) room temperature, 2 bar, 60 min; (e) room temperature, 3 bar, 75 min; (f) 50 °C, 3 bar; and (g) 100 °C, 3 bar.

on the basis of the detection of NO band at 1671 cm^{-1} in matrix-isolated studies of the reaction of laser-ablated gold with NO which was assigned to Au_xNO species,[30] it is highly likely that the NO entities with absorption bands at 1665 and 1641 cm^{-1} bridge surface Au atoms.

The band at 1808 cm^{-1} is very close to the band previously detected following adsorption of NO on Au^0/NaY[31] and reduced Au−TiO_2[19] and can be tentatively assigned to linearly bound NO on metallic Au. A band in the region 1840 cm^{-1} on Au^I/NaY has previously been assigned to $Au^I(NO)$[18] and a band at 1880 cm^{-1} on Au^0/NaY was assigned to $Au^n(NO)$ ($n \sim 0$).[31] Therefore, a shoulder at 1838 cm^{-1} is more likely to arise from NO linearly bound to electron deficient Au sites because of strong interaction with the TiO_2 support. This assignment is supported by the fact that a band in this region was detected on reduced Au−TiO_2 following a long exposure of the catalyst to NO, during which the TiO_2 surface is expected to have been reoxidized (see below). The band at 1903 cm^{-1} has previously been detected on TiO_2.[21] In addition, a band in this region has also previously been detected on Au/NaY and assigned to NO strongly interacting with ionic Au, $Au^{III}(NO^{\delta+})$.[18] It is difficult to choose between these two possibilities. However, since Au^{n+} ions can be reduced during drying and calcination,[32−34] the pretreatment history of this sample suggests that the concentration of Au^{n+} ions on this sample is very small, making the latter assignment unlikely. A band at 1860−1857 cm^{-1} is close in position to that detected on a reduced Au−TiO_2 surface after exposure to NO for a prolonged period (see Figure 3) and might be associated with metallic Au in a different chemical environment. This argument is supported by the detection of a band at ∼1880 cm^{-1} following exposure of NO to Au^0/NaY.[31] It was reported that this band was not detected when Na^I/NaY was exposed to NO. The band at 1873 cm^{-1} is just slightly below that of gas-phase NO (1876 cm^{-1}) suggesting that it is associated with NO weakly adsorbed on metallic Au. Assignment of the bands observed in this study is made in Table 1.

(ii) Calcined and Reduced Au−TiO_2. In these spectra, NO was introduced in a steady flow from the beginning of the reaction and maintained throughout the experiment. The recorded spectra in the region (∼1900−1200 cm^{-1}) for this catalyst are presented in Figure 4, and Figure 5A depicts the region (2300−2000 cm^{-1}) in expanded scale. The figures show the evolution of IR spectra as a function of time (curves a−c), pressure (curves c−d), and temperature (curves f−g). Exposure of the sample

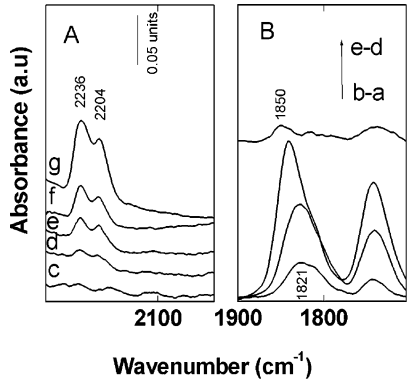

Figure 5. IR spectra of NO adsorbed on calcined and reduced Au−TiO_2. Extracted from Figure 2, A shows only the region 2300−2000 cm^{-1}. Gas (0.3% NO in He) was introduced at (c) room temperature, 1 bar, 45 min; (d) room temperature, 2 bar, 60 min; (e) room temperature, 3 bar, 75 min; (f) 50 °C, 3 bar; and (g) 100 °C, 3 bar. B is the difference spectra.

to NO for ∼15 min led to the development of the absorption bands at 1818, 1740 cm^{-1} and a broad band centered at ∼1640 cm^{-1} (Figure 4a). The behavior of this catalyst under the conditions employed can be summarized as follows:

(i) The two bands at 1818 and 1740 cm^{-1} increased in intensity with time (Figure 4a and b).

(ii) The band at 1740 cm^{-1} remained practically constant in position with time, increased NO pressure to 3 bar (Figure 4a−e), grew to saturation at this pressure (curve e), and slightly shifted to lower wavenumbers on increasing the temperature to 50 °C (curve f) and continued to shift to lower wavenumbers (1734 cm^{-1}) at 100 °C (Figure 4g). The intensity of this band (at 100 °C) decreased to ∼0.6 of the intensity at room temperature (curves e−g).

(iii) The first two bands (curves a−b) could be fitted with two Gaussian lines with the following parameters. Curve a: 1817 cm^{-1}, fwhm of ∼36 and 1740 cm^{-1}, fwhm ∼25 cm^{-1} and area ratio (1817/1740) ∼4; curve b: 1818 cm^{-1}, fwhm ∼37 cm^{-1} and 1740 cm^{-1}, fwhm ∼24 cm^{-1} and area ratio of ∼3.9. However, further reaction with NO led to the generation of complex bands (curves c−h) which would need be fitted with more than one Gaussian curve. This is shown in Figure 5B where the band maximum shifts to higher wavenumbers. This suggests that at high NO coverage, this band consists of contributions from more than one component. The band at 1818 cm^{-1} continued to grow and shifted to high wavenumbers until saturation was reached when the pressure was raised to 3 bar (curves a−e). Raising the temperature of the system to 50 and 100 °C did not affect the position or the intensity of this band (curves f−g). In contrast, the band at 1740 cm^{-1} decreased in intensity at 50 and 100 °C with a shift to lower wavenumbers (1740 → 1734 cm^{-1}).

(iv) The broad band observed at 1620 cm^{-1} decreased in intensity with time (a−c), increased NO pressure (c−e), and shifted to 1604 cm^{-1} on increasing the temperature (e−g).

(v) Two low intensity bands developed at 2236 and 2204 cm^{-1} with increased NO pressure and temperature (Figure 5A, e−g). The development and growth of bands at 2236 and 2204 cm^{-1} (Figure 5A, curves e−g) suggest that the species responsible for these bands are due to N_2O.[15,16−18,30] These species might originate from impurities in the NO gas or might be the products of the reaction of NO with Au−TiO_2. Since the bands associated with these species could only be detected long after NO exposure to Au−TiO_2 with increased NO pressure and raising the temperature of the system, it is reasonable to assume that they originate from the reaction of NO with Au−TiO_2.

The position of the bands at 1818 and 1740 cm^{-1} observed in this study identifies these species as dinitrosyl complexes, $Au(NO)_2$.[19,31] These dinitosyl complexes are sensitive to the oxidation state of the underlying $Au-TiO_2$ surface (band shifted from ~1820 cm^{-1} for reduced $Au-TiO_2$ to 1850 cm^{-1} when $Au-TiO_2$ is reoxidized, Figure 5B). In addition, there are virtually no bands in the lower wavenumber region (1500−1200 cm^{-1}) showing that the reduction of this catalyst produced a new surface with different adsorption properties or sites. The absence of NO_2 bands for the reduced catalyst (Figure 4) suggests that the contributions of NO_2 impurities in the feed gas (if any) to the surface complexes detected here (Figure 3) is negligible. The interesting points to emphasize in this study is that (i) bands characteristic of NO_x species adsorbed on TiO_2 (Figure 3) are absent on reduction of the catalyst and NO adsorption is predominantly molecular in nature (with virtually no higher NO_x or nitrogen oxo species), Figure 4. It is surprising that reduction of $Au-TiO_2$ promotes adsorption of NO onto Au containing sites (Figure 4). (ii) $Au(NO)_2$ dinitrosyl species rather than mononitrosyl complexes (Au−NO) dominate the spectra (Figure 4a−b). We have previously detected Au−NO mononitrosyl surface complexes on the freshly prepared and reduced $Au-TiO_2$ at relatively low NO coverage, and these transformed into $Au(NO)_2$ dinitrosyl complexes with increasing coverage.[19] Therefore, the reason for the detection of $Au(NO)_2$ dinitrosyl complexes and no Au−NO mononitrosyl at the beginning of the reaction might be that NO is introduced at relatively high pressure (high coverage). This is consistent with the previous interpretations of Valyon and Hall for NO on Cu surfaces[35,36] and Queeney et al.[37] for NO on Mo surfaces.

Discussion

The results presented in this paper indicate that adsorption of NO shows a remarkable sensitivity to the pretreatment of the surface. Previously, adsorption of NO on Au^I/NaY suggested that NO decomposition was promoted even at room temperature, resulting in the formation of higher nitrogen oxo surface complexes and very little molecularly adsorbed NO.[16] On the contrary, the extent of NO decomposition over Au supported on Al_2O_3, TiO_2, MgO, and SiO_2 in the temperature range 573−773 K was ~0.7% or less.[38] According to Garin,[39] metals with the intrinsic property to dissociate N−O bond are early transition elements. It is well documented that the ability of the metal to dissociate N−O bond depends on the crystallographic orientation.[40−41] However, it is not easy to relate such crystallographic texture to the data reported in this study. The detection of predominantly molecularly adsorbed NO on reduced $Au-TiO_2$ suggests that the ability of metallic Au to dissociate the N−O bond at room temperature is small. This is an important observation since catalysis by gold is currently being tested for NO_x reduction[42−46] and any new information regarding the chemisorption of NO on gold surfaces is desirable to improve our understanding of catalytic chemistry of NO_x. This observation offers an opportunity to study the mechanisms of NO_x reduction by first studying the nature of the Au−NO bond. It is also clear from the present observations that the nature of the Au−NO bond is sensitive to the state of the underlying surface, oxidized or reduced (Figures 3 and 4). This suggests that conditions can be varied at will to change the nature of this bond and to study the bonding configurations of molecularly adsorbed NO. It is also evident from the present observations that the adsorption sites of NO on $Au-TiO_2$ depend on coverage and surface temperature. This is clearly reflected in Figures 3 and 4, where, for oxidized $Au-TiO_2$, bridge-bonded NO is favored at low NO exposures (i.e., the initial adsorption of NO on this catalyst is dominated by bridging NO units, Figure 3) and these sites (bridging) are populated first. With increasing surface coverage, linearly (atop) bound NO adsorbates in different chemical environments (bands at 1873, 1860, 1838, and 1808 cm^{-1}) were detected. The intensity of the band at 1808−1810 cm^{-1} is significantly reduced compared with that found on reduced $Au-TiO_2$.[19] The bridge-bonded NO units detected at 1641 and 1665 cm^{-1} for calcined (oxidized) catalyst are not evident for reduced catalyst (Figure 4). We have no final explanation for this observation at the moment, but it might be partly because NO was introduced at relatively high pressures in the reduced sample. Bridge-bonded NO states are favored at low NO pressures. This is reflected in Figure 3g and h where at higher NO pressures an increase in the intensity of bands because of linearly bound entities is observed.

Despite the differences in the adsorption properties of $Au-TiO_2$ with pretreatment, there is a common product formed on both reduced and oxidized $Au-TiO_2$, namely, nitrous oxide, N_2O. The formation of the N−N bond found in nitrous oxide (N_2O), however, arises from different reaction mechanisms. It is generally accepted that a surface dinitrosyl complex in which two NO molecules are bound to the same surface atom is an intermediate for N_2O formation. There are two possible mechanisms for N_2O formation:[47]

(i) Dissociative mechanism

$$NO_{ads} \rightarrow N_{ads} + O_{ads} \quad (1a)$$

$$N_{ads} + NO_{ads} \rightarrow N_2O \quad (1b)$$

$$2N_{ads} \rightarrow N_2(g) \quad (1c)$$

$$2O_{ads} \rightarrow O_2(g) \quad (1d)$$

(ii) Dimerization mechanism

$$2NO_{ads} \rightarrow (NO)_2 \quad (2a)$$

$$(NO)_{2ads} \rightarrow N_2O_{ads} + O_{ads} \quad (2b)$$

$$2O_{ads} \rightarrow O_2(g) \quad (2c)$$

It is well documented in the literature that formation of N_2O from dinitrosyl surface complexes is through dimerization (reaction 2a−c).[47] Therefore in this study, the presence of the detectable amount of $Au(NO)_2$ on the surface is taken to be strong evidence for the intermediate formation of N_2O; otherwise, dissociation prior to N_2O formation is proposed (reaction 1a−c). Though spectra for reduced $Au-TiO_2$ are dominated by $Au(NO)_2$, a dissociative mechanism (reaction 1a−d) cannot be ruled out completely.

The shift in band position from 1820 to 1850 cm^{-1} (Figure 5B), which is very close in position to that found for NO adsorbed over oxidized $Au-TiO_2$ (1850−1860 cm^{-1}, Figure 3), might suggest that similar adsorption sites are involved on both surfaces. This further corroborates the assumption that the underlying oxide support material is reoxidized.

Bands associated with metallic gold, $Au(NO)_2$ species, were detected at 1510 and 1528 cm^{-1} and the positions of the bands blue shifted to 1899, 1895, and 1892 cm^{-1} when $Au^+(NO)$ was used as the adsorbing sites [30]. The shift observed in this study, from 1818 cm^{-1} for just reduced $Au-TiO_2$ to ~1850 cm^{-1} over time during which the underlying surface is expected to be reoxidized, is consistent with the earlier observations in matrix

isolation studies. This suggests that the associated Au sites in $Au(NO)_2$ with a band detected at 1850 cm^{-1} are positively polarized.[30] This is supported by the fact that a band in the same region (1850−1860 cm^{-1}) was detected for oxidized Au−TiO_2 (Figure 3). Also, dinitrosyl species in different bonding configurations were suggested to be formed in matrix isolation studies[30] and on the MoO_3 surface.[48] It is therefore reasonable to assume that Au dinitrosyl components bonded to Au sites in different chemical environments are formed on the surface, and all these contribute to the observed spectra (Figure 4). The band intensities of symmetric and asymmetric stretching vibrations of dinitrosyl complexes is related to the angle between the two NO units ($I_{asymmetric}/I_{symmetric} = \tan^2 \theta$). Therefore, the change in the relative intensities of the two bands with increased temperature is related to the changes in the angle between the two dipoles. The temperature-dependent shift in the vibrational band of a chemisorbed $(CO)_2$ on Rh−Al_2O_3 surface was modeled by electrodynamics of their interactions with the surface, considering the rocking motion of the dipoles. It was suggested that the decrease in the vibrational frequency with increasing temperature is caused by an increased electrodynamic coupling between the dynamic dipole moments of the adsorbed species with the Al_2O_3 substrate.[49] This model may explain the temperature-dependent shift of the band at 1734 cm^{-1}.

The N_2 desorption peak from dissociated NO over Au^I/NaY catalyst was reported to coincide with that for NO and N_2O.[16] Under the conditions used in this study, it is likely that N_2O is formed by diffusion of NO_{ads} or N_{ads} on the surface. The observed ν(N−N) for N_2O at 2236 cm^{-1} is slightly above the gas-phase value[50] but close to that previously reported on TiO_2.[52−53] However, ν(N−N) at 2204 cm^{-1} is close to that detected over Au^I/NaY.[16] Therefore, N_2O adsorbed on both TiO_2 and Au sites is possible. Previous detection of O_2(g) evolution from dissociated NO over Au^I/NaY was at 432 K.[16] Therefore, under the conditions used in this study, it is suggested that most O atoms from dissociated NO are still bound to the surface. Recent calculations suggest that the bond between O and Au is largely ionic in character, with electron transfer from Au s/p orbitals into empty p orbitals of O.[51] On that basis, structures such as $O_2^{\delta-}$−$Au^{\delta+}$−NO, O^-−$Au^{\delta+}$−NO, and $O^{\delta-}$−$Au^{\delta+}$−NO are highly likely. This might explain the shift in band position from 1820 to 1850 cm^{-1} with increasing NO exposure and the different chemical environments that Au sites experience (Figure 4).

Another reaction path through which N_2O can arise is the disproportionation reaction 3.[15]

$$3NO \rightarrow NO_2 + N_2O \qquad (3)$$

This reaction was also proposed for NO decomposition over Au/ZSM-5.[18] However, reaction 3 predicts the formation of equimolar amounts of N_2O and NO_2. Though this reaction is definitely important over an oxidized surface because of the detection of bands due to NO_2 adsorbed on the surface through various coordination modes (see Figure 3 and Table 1), it is definitely not a plausible choice for the reduced Au−TiO_2 (Table 1). This further suggests that the reaction path for NO on Au−TiO_2 can be varied by a choice of pretreatment and reaction conditions.

The results presented here indicate that undesired products such as NO_2 and N_2O are produced following the introduction of NO to Au−TiO_2 and that reduction of Au−TiO_2 suppressed the formation of NO_2 (Figure 4). Control of the selectivity of Au catalysts to reduce NO to N_2 without formation of these byproducts remains a challenge.

Conclusions

We have studied the effect of pretreatment on the adsorption properties of Au−TiO_2. Initial NO adsorption on oxidized Au−TiO_2 is dominated by bridging NO adsorbates (bands at 1665 and 1641 cm^{-1}). Linearly bound NO on Au was detected at high NO coverage (bands at 1873, 1860, 1838, and 1808 cm^{-1}). For this catalyst, higher nitrogen oxo species associated with TiO_2 dominate the spectra. For calcined and reduced Au−TiO_2, adsorption of NO is almost predominately molecular, dominated initially by $Au(NO)_2$ species. With increasing NO coverage, another gold component developed, resulting in peak shifting from 1818 to 1850 cm^{-1}. The Au−NO bond is sensitive to the state of underlying surface. It is proposed that $(NO)_2$ species adsorbed to Au sites in different chemical environments are formed and contribute to the observed spectra. Increasing the temperatures of the system to 50 and 100 °C, the band at 1740 cm^{-1} shifted to 1734 cm^{-1} with decrease in intensity. This is due to the increased excursion amplitude of rocking motion of $Au(NO)_2$ species. Dissociative contributions (N_2O formation) with bands at 2236 and 2204 cm^{-1} were detected and their concentrations significantly increased with an increase in temperature.

Acknowledgment. This work was financially supported by the NRF (National Research Foundation) and the University of the Witwatersrand.

References and Notes

(1) Haruta, M.; Yamada, N.; Kobayashi, T.; Iijima, S. *J. Catal*. **1989**, *115*, 301.
(2) Bond, G. C.; Thompson, D. T. *Catal. Rev.—Sci. Eng*. **1999**, *41*, 319.
(3) Valden, M.; Lai, X.; Goodman, D. W. *Science* **1998**, *281*, 1647.
(4) Valden, M.; Park, S.; Lai, X.; Goodman, D. W. *Catal. Lett*. **1998**, *56*, 7.
(5) Lee, J. Y.; Schwank, J. *J. Catal*. **1986**, *102*, 207.
(6) Bollinger, M.; Vannice, M. A. *Appl. Catal., B* **1996**, *8*, 417.
(7) Lin, S. D.; Bollinger, M.; Vannice, M. A. *Catal. Lett*. **1993**, *17*, 245.
(8) Cunnigham, D.; Tsubuta, S.; Kamijo, S.; Haruta, M. *Res. Chem. Intermed*. **1993**, *19*, 1.
(9) Tsubota, S.; Cunnigham, D. A. H.; Bando, Y.; Haruta, M. In *Preparation of Catalysts;* Elsevier: Amsterdam, 1995; Vol. VI, p 227.
(10) Park, E. D.; Lee, J. S. *J. Catal*. **1999**, *186*, 1.
(11) Galvagno, S.; Parravano, G. *J. Catal*. **1978**, *55*, 178.
(12) Cant, N. W.; Fredrickson, P. W. *J. Catal*. **1975**, *37*, 531.
(13) Konduru, M. V.; Chuang, S. S. C.; Cent, G.; Perathoner, S.; Lunsford, J. H.; Hutta, P. J.; Lin, M. J.; Windhorst, K. A. *J. Am. Chem. Soc*. **1978**, *17*, 606.
(14) Windhorst, K. A.; Lunsford, J. H. *J. Am. Chem. Soc*. **1975**, *97*, 1407.
(15) Chao, C.-C.; Lunsford, J. H. *J. Am. Chem. Soc*. **1971**, *93*, 71.
(16) Salama, T. M.; Shido, T.; Ohnishi, R.; Ichikawa, M. *J. Chem. Soc., Chem. Commun*. **1994**, 2749.
(17) Qiu, S.; Ohnishi, R.; Ichikawa, M. *J. Chem. Soc., Chem. Commun*. **1992**, 1425.
(18) Qiu, S.; Ohnishi, R.; Ichikawa, M. *J. Phys. Chem*. **1994**, *98*, 2721.
(19) Debeila, M. A.; Coville, N. J.; Scurrell, M. S.; Hearne, G. R. *Catal. Today* **2002**, *72*, 79.
(20) Hadjiivanov, K. I. *Catal. Rev.—Sci. Eng*. **2000**, *42*, 71.
(21) Debeila, M. A.; Coville, N. J.; Scurrell, M. S.; Hearne, G. R. submitted for publication.
(22) Anderson, J. A.; Rochester, C. H. *J. Chem. Soc., Faraday Trans*. **1991**, *87*, 1485.
(23) Elhamdaoui, A.; Bergeret, G.; Massardier, J.; Primet, M.; Renouprez, A. *J. Catal*. **1994**, *148*, 47.
(24) Krishnamurthy, R.; Chuang, S.; Balakos, M. *J. Catal*. **1995**, *157*, 512.
(25) Tomishige, K.; Asakura, K.; Iwasawa, Y. *J. Catal*. **1995**, *157*, 472.
(26) Sica, A. M.; Dos Santos, J. H. Z.; Baibich, I. M.; Gigola, E. C. *J. Mol. Catal. A* **1999**, *137*, 287.
(27) Lizuka, T.; Lunsford, J. H. *J. Mol. Catal*. **1980**, *8*, 391.
(28) Bartram, M. E.; Koel, B. E.; Carter, E. A. *Surf. Sci*. **1989**, *219*, 467.

(29) Conrad, H.; Ertl, G.; Kuppers, J.; Latta, E. E. *Surf. Sci*. **1977**, *65*, 235.
(30) Citra, A.; Wang, X.; Andrews, L. *J. Phys. Chem. A* **2002**, *106*, 3287.
(31) Salama, T. M.; Ohnishi, R.; Shido, T.; Ichikawa, M. *J. Catal*. **1996**, *162*, 169.
(32) Su, Y.-S.; Lee, M.-Y.; Lin, S. D. *Catal. Lett*. **1999**, *57*, 49.
(33) Schumacher, B.; Plzak, V.; Kinne, M.; Behm, R. J. *Catal. Lett*. **2003**, *89*, 109.
(34) Soares, J. M. C.; Morrall, P.; Crossley, A.; Harris, P.; Bowker, M. *J. Catal*. **2003**, *219*, 17.
(35) Valyon, J.; Hall, H. K. *Stud. Surf. Sci. Catal*. **1993**, *74*, 1339.
(36) Valyon, J.; Hall, H. K. *J. Phys. Chem*. **1993**, *97*, 1204.
(37) Queeny, K. T.; Friend, C. M. *J. Chem. Phys*. **1997**, *107*, 6432.
(38) Solymosi, F.; Bansagi, T.; Zakar, T. S. *Phys. Chem. Chem. Phys*. **2003**, *5*, 4724.
(39) Garin, F. *Appl. Catal*., *A* **2001**, *222*, 183.
(40) Root, T. W.; Fisher, G. B.; Schmidt, L. D. *J. Chem. Phys*. **1986**, *85*, 4679.
(41) Villarrubia, J. S.; Ho, W. *J. Chem. Phys*. **1987**, *87*, 750.
(42) Ueda, A.; Haruta, M. *Gold Bull*. **1999**, *32*, 3.
(43) Kung, M. C.; Lee, J. H.; Chukung, A.; Kung, H. H. *Stud. Surf. Sci. Catal*. **1996**, *101*, 701.
(44) Kung, M. C.; Bethke, K. A.; Lee, J.-H.; Kung, H. H. *Appl. Surf. Sci*. **1997**, *121/122*, 261.
(45) Ueda, A.; Haruta, M. *Appl. Catal*., *B* **1998**, *18*, 115.
(46) Bamwenda, G. R.; Obushi, A.; Ogata, A.; Oi, J.; Kushiyama, S.; Yagit, H.; Mizino, K. *Stud. Surf. Sci. Catal*. **1999**, *121*, 263.
(47) Panja, C.; Koel, B. E. *J. Phys. Chem. A* **2000**, *104*, 2486.
(48) Remediakis, I. N.; Kaxiras, E.; Chen, M.; Friend, C. M. *J. Chem. Phys*. **2003**, *118*, 6046.
(49) Antoniewicz, P. R.; Cavanagh, R. R.; Yates, J. T., Jr. *J. Chem. Phys*. **1980**, *73*, 3456.
(50) Laane, J.; Ohlen, J. R. *Prog. Inorg. Chem*. **1980**, *27*, 465.
(51) Liu, Z.-P.; Hu, P.; Alavi, A. *J. Am. Chem. Soc*. **2002**, *124*, 14770.
(52) Ramis, G.; Busca, G.; Lorenzelli, V.; Forzatti, P. *Appl. Catal*. **1990**, *64*, 243.
(53) Cant, N. W.; Cole, J. R. *J. Catal*. **1992**, *134*, 317.